

University of Bergen, Department of Physics

Scientific/Technical Report No. 1999-09

ISSN 0803-2696

hep-ph/9911295

November 1999

Multiple Higgs Production and Measurement of Higgs Trilinear Couplings in the MSSM

P. Osland ^a and P. N. Pandita ^b

^a *Department of Physics, University of Bergen, Allégaten 55, N-5007 Bergen, Norway*

^b *Department of Physics, North Eastern Hill University, Shillong 793 022, India*

Multiple Higgs Production and Measurement of Higgs Trilinear Couplings in the MSSM¹

P. Osland^a and P. N. Pandita^b

^aDepartment of Physics, University of Bergen, N-5007 Bergen, Norway

^b Department of Physics, North Eastern Hill University,
Shillong 793 022, India

Abstract

An elementary Higgs boson, which is the remnant of the spontaneous symmetry breaking mechanism in the Standard Model, remains one of the most elusive particles. If a Higgs boson candidate is found at future accelerators, it becomes necessary to determine its properties, beyond the mass, production cross section and decay rates. The other crucial properties relate to the self-couplings of the Higgs boson, which are necessary to reconstruct the Higgs potential, and thereby confirm the mechanism of spontaneous symmetry breaking. In this paper we review the question of the measurability of some of the trilinear couplings of the neutral Higgs bosons of the Minimal Supersymmetric Standard Model at a high-energy e^+e^- collider.

1 Introduction

The Higgs mechanism, which is responsible for the generation of all particle masses in the Standard Model (SM), is as yet an experimentally untested mechanism. This mechanism of mass generation leaves behind a remnant in the form of scalar particle(s), the Higgs boson(s), which has eluded the experimental search so far. The Higgs particle is expected to be discovered at the LHC, if not at LEP2 [1]. Current estimates from precision electroweak data [2] suggest that it is rather light. Although a light Higgs particle would be consistent with the Standard Model, it is natural only in a supersymmetric framework [3]. The minimal version of the Supersymmetric Standard Model (MSSM) contains two Higgs doublets (H_1, H_2) with opposite hypercharges [4]: $Y(H_1) = -1$, $Y(H_2) = +1$, so as to generate masses for up- and down-type quarks (and leptons), and to cancel triangle gauge anomalies. After spontaneous symmetry breaking induced by the neutral components of H_1 and H_2 obtaining vacuum expectation values, $\langle H_1 \rangle = v_1$, $\langle H_2 \rangle = v_2$, $\tan \beta = v_2/v_1$, the MSSM contains two neutral CP -even (h, H), one neutral CP -odd (A), and two charged (H^\pm) Higgs bosons. Because of gauge invariance and supersymmetry, all the Higgs masses and the Higgs couplings in the MSSM can be described (at tree level) in terms of only two parameters, which are usually chosen to be $\tan \beta$ and m_A , the mass of the CP -odd Higgs boson. Once a light Higgs boson is discovered, a detailed measurement of its branching ratios should, in principle, enable one to distinguish between a SM Higgs boson and the lightest MSSM Higgs boson.

¹To appear in the *Proceedings of XIVth International Workshop: High Energy Physics and Quantum Field Theory*, Moscow, Russia, 27 May – 2 June 1999.

Apart from the large number of Higgs bosons in the minimal version of the supersymmetric standard model, there is more to the MSSM Higgs sector than the branching ratios. For a complete analysis of the Higgs sector, one should also measure the trilinear and quartic self-couplings of the Higgs boson, which in the MSSM are determined (at the tree level) by the gauge couplings. The measurability of trilinear couplings involving the light Higgs boson was investigated by Djouadi, Haber and Zerwas [5]. In this preliminary study, it was concluded that the trilinear couplings λ_{Hhh} and λ_{hhh} , where h and H denote the two neutral, CP -even Higgs bosons, could be measured at a high-energy e^+e^- linear collider. A more detailed study, including the squark mixing, of the measurability of the trilinear Higgs couplings was carried out in [6]. Recently, the leading two-loop effects have also been incorporated in the calculations [7].

All the trilinear self-couplings of the physical Higgs particles can be predicted theoretically (at the tree level) in terms of m_A and $\tan\beta$. Once a light Higgs boson is discovered, the measurement of these trilinear couplings can be used to reconstruct the Higgs potential of the MSSM. This will go a long way in establishing the Higgs mechanism as the basic mechanism of spontaneous symmetry breaking in gauge theories.

We have considered in detail [6] the question of the possible measurements of some of the trilinear Higgs couplings of the MSSM at a high-energy e^+e^- linear collider that will operate at an energy of 500 GeV with an integrated luminosity per year of $\mathcal{L}_{\text{int}} = 500 \text{ fb}^{-1}$ [8]. We focus on the trilinear Higgs couplings λ_{Hhh} and λ_{hhh} , involving the CP -even Higgs bosons. They are rather small with respect to the corresponding trilinear coupling $\lambda_{hhh}^{\text{SM}}$ in the SM (for a given mass of the lightest Higgs boson m_h), unless m_h is close to the upper value (the decoupling limit).

2 Trilinear Higgs couplings

In units of $gm_Z/(2\cos\theta_W) = (\sqrt{2}G_F)^{1/2}m_Z^2$, the *tree-level* trilinear Higgs couplings of the MSSM, that we shall discuss, are given by [4]:

$$\lambda_{hhh}^0 = 3\cos 2\alpha \sin(\beta + \alpha), \quad (1)$$

$$\lambda_{Hhh}^0 = 2\sin 2\alpha \sin(\beta + \alpha) - \cos 2\alpha \cos(\beta + \alpha), \quad (2)$$

where α is the mixing angle in the CP -even Higgs sector, which is determined by the parameters of the CP -even Higgs boson mass matrix.

The trilinear Higgs couplings λ_{Hhh} and λ_{hhh} of the neutral Higgs bosons in the Minimal Supersymmetric Standard Model (MSSM), Eqs. (1) and (2), involve the CP -even Higgs bosons h and H . These trilinear couplings can be measured through the multiple production of the Higgs bosons at high-energy e^+e^- colliders. The relevant production mechanisms that we shall consider are the production of the heavier CP -even Higgs boson via $e^+e^- \rightarrow ZH$, in association with the CP -odd Higgs boson (A) in $e^+e^- \rightarrow AH$, or via the fusion process $e^+e^- \rightarrow \nu_e \bar{\nu}_e H$, with H subsequently decaying through $H \rightarrow hh$. The multiple production of the light Higgs boson through Higgs-strahlung of H , and through production of H in association with the CP -odd Higgs boson can be used to extract the trilinear Higgs coupling λ_{Hhh} . The non-resonant fusion mechanism for multiple h production, $e^+e^- \rightarrow \nu_e \bar{\nu}_e hh$, involves two trilinear Higgs couplings, λ_{Hhh} and λ_{hhh} , and is useful

for extracting λ_{hhh} . For the extraction of other MSSM trilinear Higgs couplings, λ_{HHh} , λ_{HHH} , λ_{hAA} , and λ_{HAA} , at e^+e^- colliders, see [7].

At the tree level, the CP-even Higgs boson h is rather light, and $m_h \leq m_Z$ holds. However, there are large radiative corrections to this result and a new bound is set, $m_h \leq 135$ GeV. The dominant one-loop radiative corrections are proportional to $(m_t/m_W)^4$, and to a set of complicated functions depending on the squark masses [9, 10]. Recently, the dominant two-loop radiative corrections [11] to the Higgs sector have been evaluated. The two-loop contributions yield a large correction to the one-loop result, and as a consequence m_h is reduced by up to ~ 20 GeV, which is particularly important for low values of $\tan\beta$. In Fig. 1 we plot the two-loop corrected mass of the lightest Higgs boson as a function of m_A and $\tan\beta$ for two values of the mixing parameters A and μ , as indicated².

We shall include one-loop radiative corrections [9, 10], as well as the leading two-loop corrections [11], to the Higgs sector in our calculations. In particular, we take into account [6] the parameters A and μ , the soft supersymmetry breaking trilinear parameter and the bilinear Higgs(ino) parameter in the superpotential. These parameters determine the stop masses,

$$m_{t_{1,2}}^2 = m_t^2 + \tilde{m}^2 \pm m_t(A + \mu \cot\beta) \quad (3)$$

which enter through the radiative corrections to the Higgs masses as well as to the Higgs trilinear couplings.

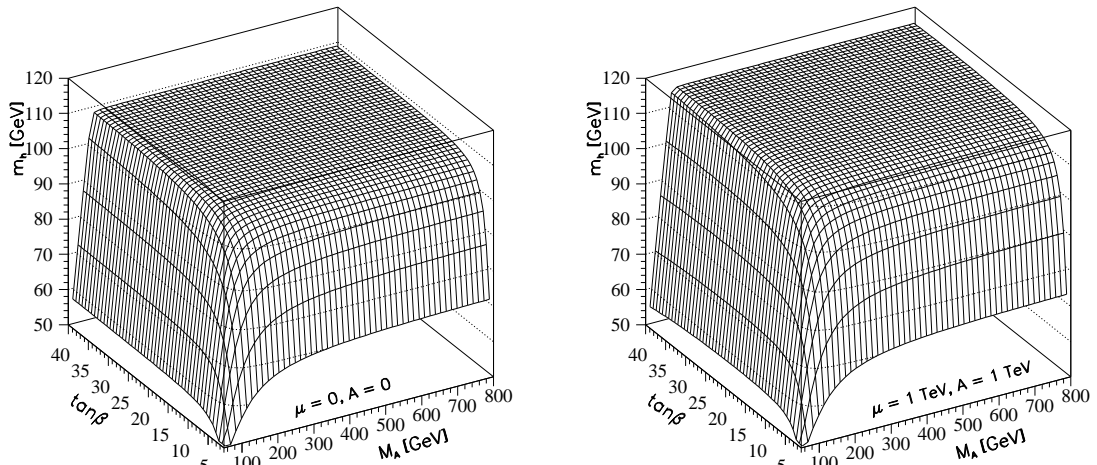


Figure 1. Mass of the lightest CP-even Higgs boson, m_h vs. m_A and $\tan\beta$. Two cases are considered for the mixing parameters μ and A , as indicated. Two-loop corrections are included [11].

The trilinear couplings depend significantly on m_A , and thus also on m_h . This is shown in Fig. 2, where we compare λ_{HHh} , λ_{hhh} and λ_{hAA} for two different values of $\tan\beta$. For a given value of m_h , the values of these couplings significantly depend on the soft supersymmetry-breaking trilinear parameter A , as well as on μ .

²The LEP experiments have obtained strong lower bounds on the mass of the lightest Higgs boson, and are beginning to rule out significant parts of the small- $\tan\beta$ parameter space. ALEPH finds a lower limit of $m_h > 72.2$ GeV, irrespective of $\tan\beta$, and a limit of ~ 88 GeV for $1 < \tan\beta \lesssim 2$ [12].

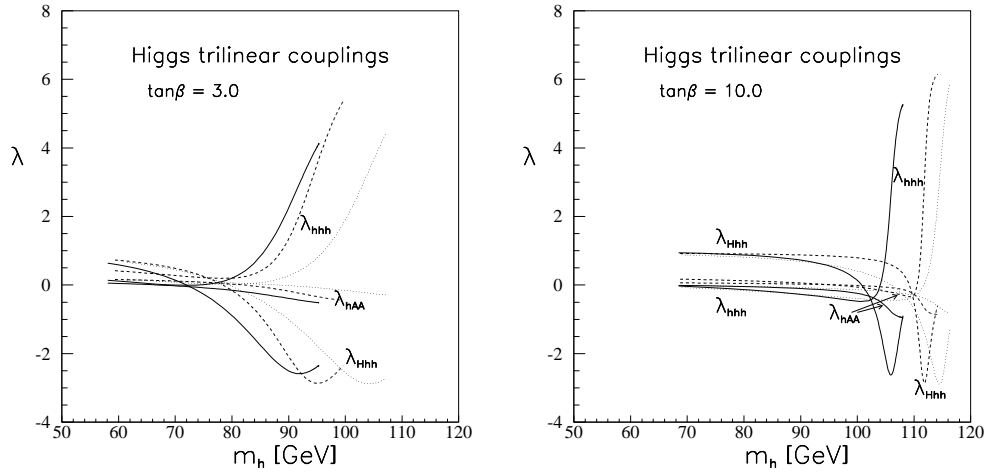


Figure 2. Trilinear Higgs couplings λ_{Hhh} , λ_{hhh} and λ_{hAA} as functions of m_h for $\tan \beta = 3.0$ and $\tan \beta = 10.0$. Each coupling is shown for $\tilde{m} = 1$ TeV, and for three cases of the mixing parameters: no mixing ($A = 0$, $\mu = 0$, solid), mixing with $A = 1$ TeV and $\mu = -1$ TeV (dotted), as well as $A = 1$ TeV and $\mu = 1$ TeV (dashed).

As is clear from Fig. 2, at low values of m_h , the MSSM trilinear couplings are rather small. For some value of m_h the couplings λ_{Hhh} and λ_{hhh} start to increase in magnitude, whereas λ_{hAA} remains small.

3 Production mechanisms

The dominant mechanisms for the production of multiple CP -even light Higgs bosons is through the processes

$$\left. \begin{aligned} e^+e^- &\rightarrow ZH, AH \\ e^+e^- &\rightarrow \nu_e \bar{\nu}_e H \end{aligned} \right\}, \quad H \rightarrow hh, \quad (4)$$

shown in Fig. 3. The heavy Higgs boson H can be produced by H -strahlung, in association with A , and by the resonant WW fusion mechanism. All the diagrams of Fig. 3 involve the trilinear coupling λ_{Hhh} .

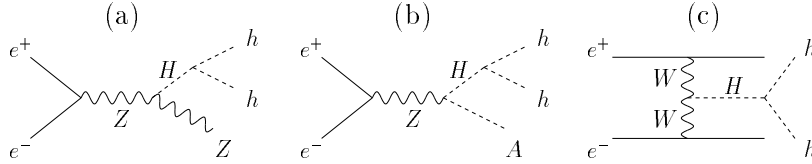


Figure 3. Feynman diagrams for the resonant production of hh final states in e^+e^- collisions.

A background to the processes (4) comes from the production of the pseudoscalar A in association with h and its subsequent decay to hZ

$$e^+e^- \rightarrow hA, \quad A \rightarrow hZ, \quad (5)$$

leading to Zhh final states.

Another mechanism for hh production is double Higgs-strahlung in the continuum with a Z boson in the final state,

$$e^+e^- \rightarrow Z^* \rightarrow Zhh. \quad (6)$$

Finally, there is also a mechanism for the multiple production of the lightest Higgs boson through non-resonant WW fusion in the continuum:

$$e^+e^- \rightarrow \bar{\nu}_e \nu_e W^* W^* \rightarrow \bar{\nu}_e \nu_e hh, \quad (7)$$

as shown in Fig. 4.

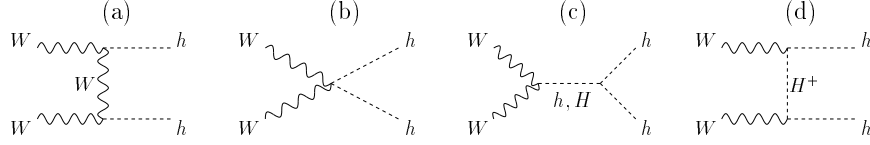


Figure 4. Feynman diagrams for the non-resonant WW fusion mechanism for the production of hh states in e^+e^- collisions.

It is important to note that all the diagrams of Fig. 3 involve the trilinear coupling λ_{Hhh} only. In contrast, the non-resonant analogues of Figs. 3a, 3b and 3c (or 4c) involve both the trilinear Higgs couplings λ_{Hhh} and λ_{hhh} .

3.1 Higgs-strahlung and associated production of H

The dominant source for the production of multiple light Higgs bosons in e^+e^- collisions is through the production of the heavier CP -even Higgs boson H either via Higgs-strahlung or in association with A , followed, if kinematically allowed, by the decay $H \rightarrow hh$.

In Fig. 5 we plot the relevant cross sections [13, 14] for the e^+e^- centre-of-mass energy $\sqrt{s} = 500$ GeV, as functions of the Higgs mass m_H and for $\tan \beta = 3.0$. For a fixed value of m_H , there is seen to be a significant sensitivity to the squark mixing parameters μ and A . We have here taken $\tilde{m} = 1$ TeV, a value which is adopted throughout, except where otherwise specified.

A measurement of the decay rate $H \rightarrow hh$ directly yields λ_{Hhh}^2 . But this is possible only if the decay is kinematically allowed, and the branching ratio is sizeable (but not too close to unity). In Fig. 6 we show the branching ratios (at $\tan \beta = 3.0$) for the main decay modes of the heavy CP -even Higgs boson as a function of the H mass [15]. Apart from the hh decay mode, the other important decay modes are $H \rightarrow b\bar{b}$, WW^* , ZZ^* . For increasing values of $\tan \beta$ (but fixed m_h), the Hhh coupling gradually gets weaker (Fig. 2), and hence the prospects for measuring λ_{Hhh} diminish. Also, the decay rates can change significantly with \tilde{m} , the over-all squark mass scale (see Fig. 6).

There is a sizeable region in the m_A - $\tan \beta$ plane where the decay $H \rightarrow hh$ is kinematically forbidden, which is shown in Fig. 7 as an egg-shaped region at the upper left of the plot. The boundary of the region depends crucially on the precise Higgs mass values.

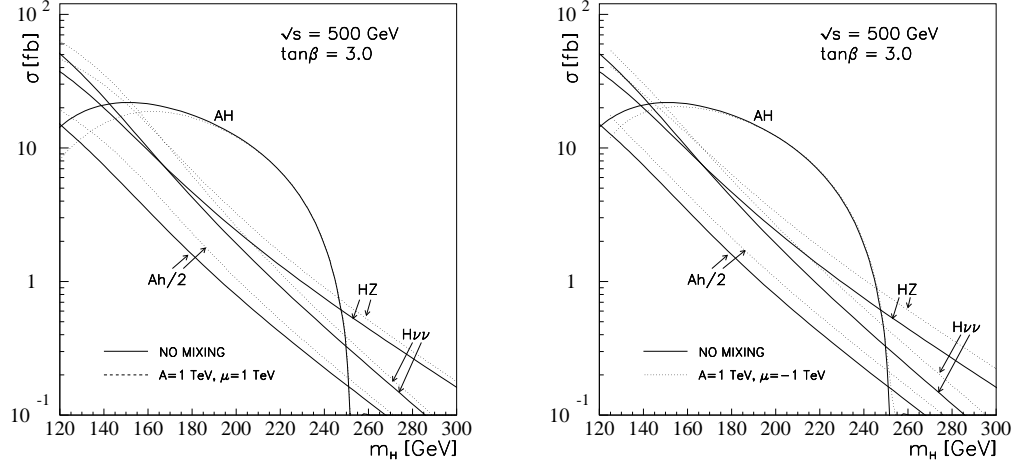


Figure 5. Cross sections for the production of the heavy Higgs boson H in e^+e^- collisions, and for the background process in which Ah is produced. Solid curves are for no mixing, $A = 0$, $\mu = 0$. Dashed and dotted curves refer to mixing.

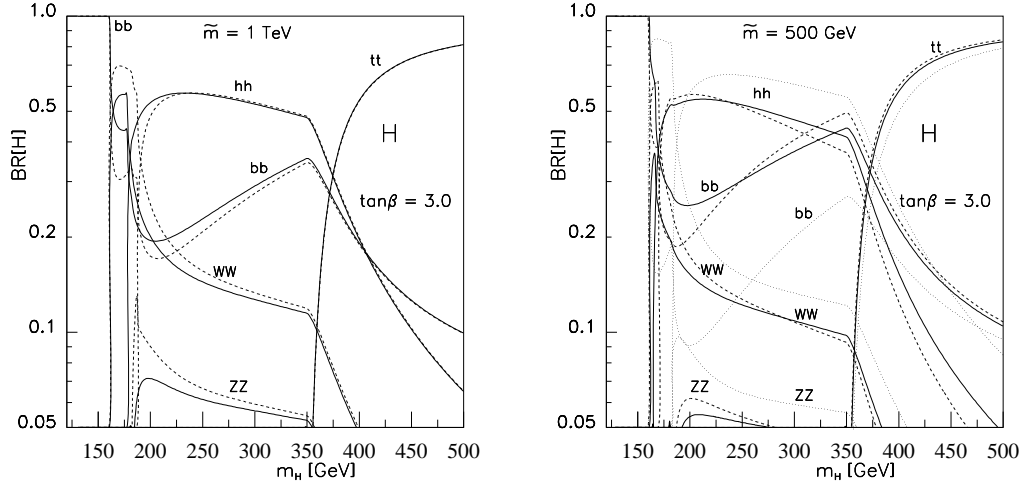


Figure 6. Branching ratios for the decay modes of the CP -even heavy Higgs boson H , for $\tan\beta = 3.0$ and \tilde{m} equal to 1 TeV or 500 GeV, as indicated. Solid curves are for no mixing, $A = 0$, $\mu = 0$. For $\tilde{m} = 1$ TeV, the dashed curves refer to $A = 1$ TeV and $\mu = 1$ TeV, whereas for $\tilde{m} = 500$ GeV, the dashed (dotted) curves refer to $A = 500$ GeV (800 GeV) and $\mu = 1$ TeV (800 GeV).

This is illustrated by comparing two cases of mixing parameters A and μ . We also display the regions where the $H \rightarrow hh$ branching ratio is in the range 0.1–0.9. Obviously, in the forbidden region, the λ_{Hhh} cannot be determined from resonant production.

3.2 Double Higgs-strahlung

As discussed above, for small and moderate values of $\tan\beta$, a study of decays of the heavy CP -even Higgs boson H provides a means of determining the triple-Higgs coupling λ_{Hhh} . For the purpose of extracting the coupling λ_{hhh} , non-resonant processes involving two-Higgs (h) final states must be considered. The Zhh final states produced in the

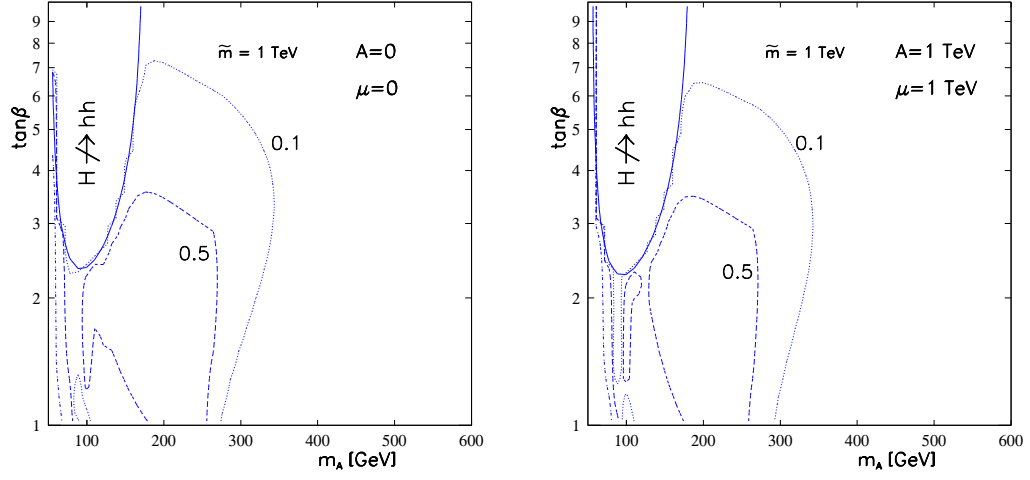


Figure 7. The region in the m_A - $\tan \beta$ plane where the decay $H \rightarrow hh$ is kinematically forbidden is indicated by a solid line contour. Also given are contours at which the branching ratio equals 0.1 (dotted), 0.5 (dashed) and 0.9 (dash-dotted, far left).

non-resonant double Higgs-strahlung $e^+e^- \rightarrow Zh h$, and whose cross section involves the coupling λ_{hhh} , could provide one possible opportunity.

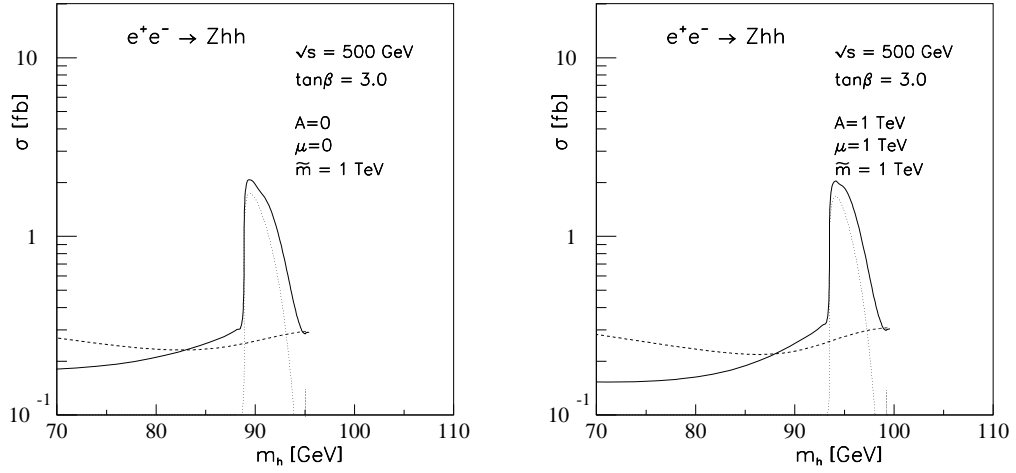


Figure 8. Cross section $\sigma(e^+e^- \rightarrow Zh h)$ as a function of m_h . The dotted curve is the resonant production, the dashed curve gives the decoupling limit [16].

However, the non-resonant contribution to the Zhh cross section is rather small, as is shown in Fig. 8 for $\sqrt{s} = 500$ GeV, $\tan \beta = 3.0$, and $\tilde{m} = 1$ TeV. At low values of m_h , the decay $H \rightarrow hh$ is kinematically forbidden. This is followed by an increase of the trilinear couplings.

Since the non-resonant part of the cross section, which depends on λ_{hhh} , is rather small, this channel is not suitable for a determination of λ_{hhh} [5].

3.3 Fusion mechanism for multiple- h production

A two-Higgs (hh) final state can also result from the WW fusion mechanism in e^+e^- collisions. There is a resonant contribution (through H) and a non-resonant one.

The resonant WW fusion cross section for $e^+e^- \rightarrow H\bar{\nu}_e\nu_e$ [17] is plotted in Fig. 5 for the centre-of-mass energy $\sqrt{s} = 500$ GeV, and for $\tan\beta = 3.0$, as a function of m_H .

Besides the resonant WW fusion mechanism for the multiple production of h bosons, there is also a non-resonant WW fusion mechanism:

$$e^+e^- \rightarrow \nu_e\bar{\nu}_e hh, \quad (8)$$

through which the same final state of two h bosons can be produced. The cross section for this process (see Fig. 4), can be written in the effective WW approximation as a WW cross section, at invariant energy squared $\hat{s} = xs$, folded with the WW “luminosity” [18]. Thus,

$$\sigma(e^+e^- \rightarrow \nu_e\bar{\nu}_e hh) = \int_{\tau}^1 dx \frac{dL}{dx} \hat{\sigma}_{WW}(x), \quad (9)$$

where $\tau = 4m_h^2/s$, and

$$\frac{dL(x)}{dx} = \frac{G_F^2 m_W^4}{2} \left(\frac{1}{2\pi^2} \right)^2 \frac{1}{x} \left\{ (1+x) \log \frac{1}{x} - 2(1-x) \right\}. \quad (10)$$

The WW cross section receives contributions from several amplitudes, according to the diagrams (a)–(d) in Fig. 4, only one of which is proportional to λ_{hhh} . We have evaluated these contributions [6], following the approach of Ref. [19], ignoring transverse momenta everywhere except in the W propagators. Our approach also differs from that of [5] in that we do not project out the longitudinal degrees of freedom of the intermediate W bosons.

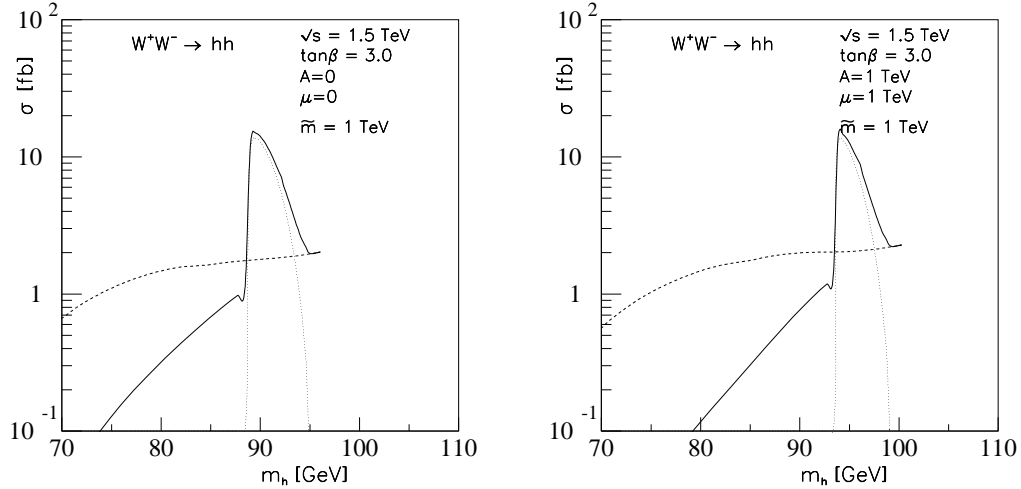


Figure 9. Cross section $\sigma(e^+e^- \rightarrow \nu_e\bar{\nu}_e hh)$ (via WW fusion) as a function of m_h . The dotted curve is the resonant production, the dashed curve gives the decoupling limit.

We show in Fig. 9 the resulting WW fusion cross section, at $\sqrt{s} = 1.5$ TeV, and for $\tilde{m} = 1$ TeV. The structure is reminiscent of Fig. 8, and the reasons for this are the same. Notice, however, that the scale is different. Since this is a fusion cross section, it grows logarithmically with energy.

For high values of m_h we see that there is a moderate contribution to the cross section from the non-resonant part. For a lower squark mass scale \tilde{m} , the situation is rather similar, except that the cross section peak (from resonant production) gets shifted to a higher Higgs mass, m_h .

4 Sensitivity to λ_{Hhh} and λ_{hhh}

We are now ready to combine the results and discuss in which parts of the m_A – $\tan\beta$ plane one might hope to measure the trilinear couplings λ_{Hhh} and λ_{hhh} . In Figs. 10 and 11 we have identified regions according to the following criteria [5, 6]:

- (i) Regions where λ_{Hhh} might become measurable are identified as those where $\sigma(H) \times \text{BR}(H \rightarrow hh) > 0.1$ fb (solid), while simultaneously $0.1 < \text{BR}(H \rightarrow hh) < 0.9$ [see Figs. 6–7]. In view of the recent, more optimistic, view on the luminosity that might become available, we also give the corresponding contours for 0.05 fb (dashed) and 0.01 fb (dotted).
- (ii) Regions where λ_{hhh} might become measurable are those where the *continuum* $WW \rightarrow hh$ cross section [Eq. (9)] is larger than 0.1 fb (solid). Also shown are contours at 0.05 (dashed) and 0.01 fb (dotted).

We have excluded from the plots the region where $m_h < 72.2$ GeV [12]. This corresponds to low values of m_A and low $\tan\beta$.

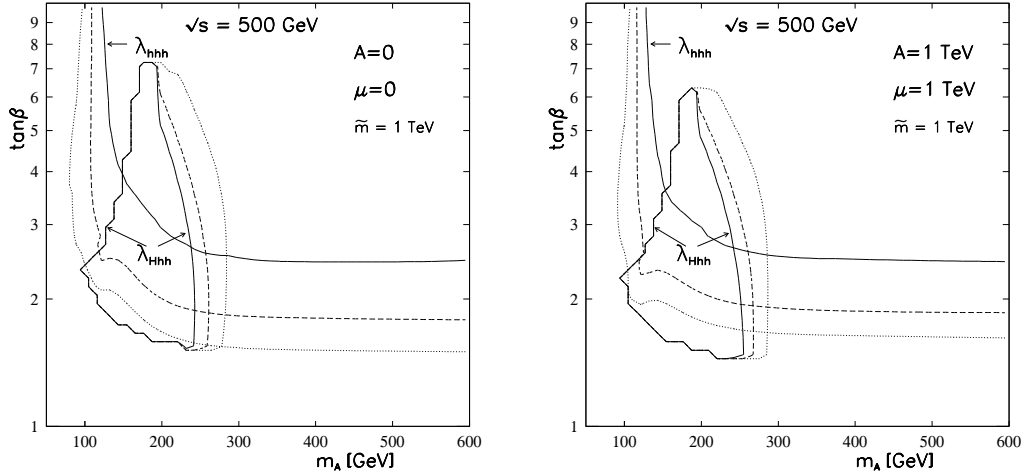


Figure 10. Regions where trilinear couplings λ_{Hhh} and λ_{hhh} might be measurable at $\sqrt{s} = 500$ GeV. Inside contours labelled λ_{Hhh} , $\sigma(H) \times \text{BR}(H \rightarrow hh) > 0.1$ fb (solid), while $0.1 < \text{BR}(H \rightarrow hh) < 0.9$. Inside (to the right or below) contour labelled λ_{hhh} , the *continuum* $WW \rightarrow hh$ cross section exceeds 0.1 fb (solid). Analogous contours are given for 0.05 (dashed) and 0.01 fb (dotted). Two cases of squark mixing are considered, as indicated.

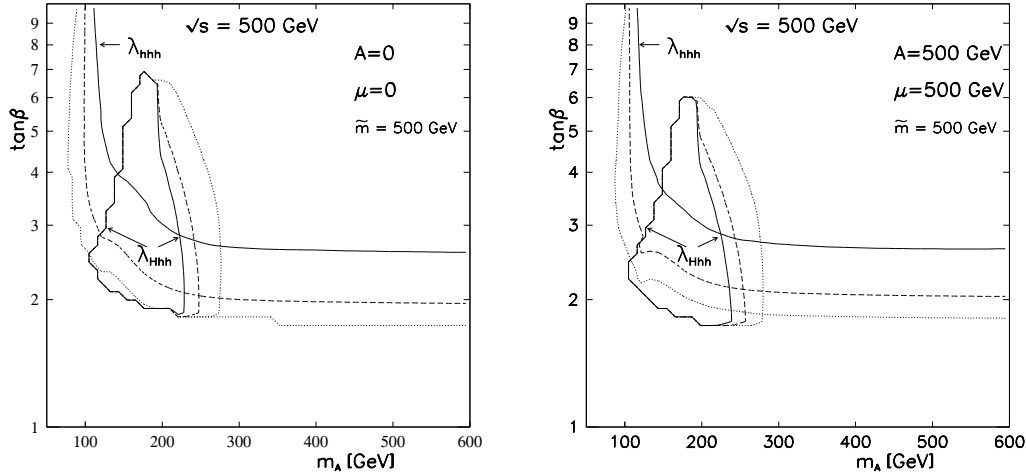


Figure 11. Similar to Fig. 10 for $\tilde{m} = 500$ GeV.

These cross sections are small, the measurements are not going to be easy. With an integrated luminosity of 500 fb^{-1} , the contours at 0.1 fb correspond to 50 events per year. This will be reduced by efficiencies, but should indicate the order of magnitude that can be reached. For the case of the SM Higgs, the backgrounds have been studied [20] and the measurements appear feasible.

With increasing luminosity, the region where λ_{Hhh} might be accessible, extends somewhat to higher values of m_A . Note the steep edge around $m_A \simeq 200$ GeV, where increased luminosity does not help. This is determined by the vanishing of $\text{BR}(H \rightarrow hh)$, as seen in Fig. 7. The coupling $\lambda_{h hh}$ is accessible in a much larger part of this parameter space.

The precise region in the $\tan \beta - m_A$ plane, in which these couplings might be accessible, depends on details of the model. As a further illustration of this point, we show in Fig. 11 the corresponding plots for a squark mass parameter $\tilde{m} = 500$ GeV.

5 Conclusions

We have reviewed the updated results of a detailed investigation [6] of the possibility of measuring the MSSM trilinear couplings λ_{Hhh} and $\lambda_{h hh}$ at an e^+e^- collider, focussing in detail on the importance of mixing in the squark sector, as induced by the trilinear coupling A and the bilinear coupling μ . As compared with our earlier work, we here use two-loop results for the Higgs masses [11]. The two-loop results for the Higgs masses have considerably less dependence on squark mixing.

As a result of the two-loop Higgs masses being less sensitive to squark mixing, the regions in the $m_A - \tan \beta$ plane that are accessible for studying λ_{Hhh} and $\lambda_{h hh}$ are more stable than was the case for the one-loop results.

This research was supported by the Research Council of Norway, and (PNP) by the University Grants Commission, India under project number 10-26/98(SR-I).

References

- [1] P.A. McNamara, Proceedings of the 29th International Conference on High Energy Physics (ICHEP '98), Vancouver 1998, eds. A. Ashtbury, D. Axen and J. Robinson, World Scientific (1999), p. 1303. See also P. M. Zerwas, *Acta Phys. Polon.* **B30** (1999) 1871.
- [2] G. Altarelli, R. Barbieri, F. Caravaglios, *Int. J. Mod. Phys.* **A13** (1998) 1031.
- [3] For reviews, see H.-P. Nilles, *Phys. Rep.* **110**, 1 (1984); H. E. Haber and G. L. Kane, *Phys. Rep.* **C117**, 75 (1985); R. Barbieri, *Riv. Nuovo Cimento* **11** No. 4, p. 1 (1988).
- [4] J. F. Gunion, H. E. Haber, G. Kane and S. Dawson, *The Higgs Hunter's Guide*, Addison-Wesley, New York, 1990.
- [5] A. Djouadi, H. E. Haber and P. M. Zerwas, *Phys. Lett.* **B375**, 203 (1996) and Erratum, to be published.
- [6] P. Osland and P. N. Pandita, *Phys. Rev. D* **59** (1999) 055013; Invited paper, *VIIIth UNESCO St. Petersburg International School of Physics*, May 25 – June 4, 1998 (to be published in the Proceedings) (Archive: hep-ph/9902270); P. Osland, *Acta Phys. Polon.* **B30** (1999) 1967.
- [7] A. Djouadi, W. Kilian, M. Muhlleitner and P. M. Zerwas, *Eur. Phys. J.* **C10** (1999) 45.
- [8] M. Tigner, B. Wiik and F. Willeke, *Particle Accel. Conf. IEEE* (1991) 2910; S. Kuhlman *et al.* (The NLC ZDR Design Group and the NLC Physics Working Groups), *Physics and Technology of the Next Linear Collider: A Report Submitted to Snowmass '96*, BNL 52-502, FERMILAB-PUB-96/112, LBNL-PUB-5425, SLAC-Report-485, UCRL-ID-124160, UC-414 (June 1996); H. Murayama and M. E. Peskin, *Ann. Rev. Nucl. Part. Sci.* **46** (1996) 533; *e+e- Linear Colliders: Physics and Detector Studies*, R. Settles, editor, Proceedings, workshops, ECFA/DESY, Frascati, London, Munich, Hamburg, DESY-97-123E, 1997.
- [9] J. Ellis, G. Ridolfi and F. Zwirner, *Phys. Lett.* **B257**, 83 (1991); Y. Okada, M. Yamaguchi and T. Yanagida, *Prog. Theor. Phys.* **85**, 1 (1991); H. E. Haber and R. Hempfling, *Phys. Rev. Lett.* **66**, 1815 (1991); J. Ellis, G. Ridolfi and F. Zwirner, *Phys. Lett.* **B262**, 477 (1991); R. Hempfling and A. H. Hoang, *Phys. Lett.* **B331**, 99 (1994); M. Carena, J.R. Espinosa, M. Quirós and C.E.M. Wagner, *Phys. Lett.* **B355**, 209 (1995); M. Carena, M. Quirós and C.E.M. Wagner, *Nucl. Phys.* **B461**, 407 (1996); S. Heinemeyer, W. Hollik and G. Weiglein, *Phys. Rev.* **D58**, 091701 (1998).
- [10] V. Barger, M. S. Berger, A. L. Stange and R. J. N. Phillips, *Phys. Rev.* **D45**, 4128 (1992).

- [11] S. Heinemeyer, W. Hollik and G. Weiglein, Eur. Phys. J. **C9** (1999) 343; hep-ph/9812320; Phys. Lett. **B455** (1999) 179.
- [12] R. Barate *et al.* (ALEPH Collaboration), Phys. Lett. **B 440** (1998) 419.
- [13] G. Pócsik and G. Zsigmond, Z. Phys. **C10**, 367 (1981).
- [14] J. F. Gunion, L. Roszkowski, A. Turski, H. E. Haber, G. Gamberini, B. Kayser, S. F. Novaes, F. Olness and J. Wudka, Phys. Rev. **D38**, 3444 (1988).
- [15] For a review, see A. Djouadi, J. Kalinowski and P. M. Zerwas, Z. Phys. **C70**, 435 (1996).
- [16] H. E. Haber, in Proceedings of the Conference on *Perspectives for Electroweak Interactions in e^+e^- Collisions*, Ringberg (Tegernsee), Germany, 1995; ed. B. A. Kniehl (World Scientific, Singapore, 1995) p. 219.
- [17] A. Djouadi, D. Haidt, B. A. Kniehl, B. Mele and P. M. Zerwas, in Proceedings, Workshop on e^+e^- Collisions at 500 GeV: *The Physics Potential*, Munich-Annecy-Hamburg (DESY 92-123 A, Hamburg, 1992).
- [18] R. N. Cahn and S. Dawson, Phys. Lett. **B136**, 196 (1984); S. Dawson, Nucl. Phys. **B249**, 42 (1984); M. Chanowitz and M. K. Gaillard, Phys. Lett. **B142**, 85 (1984); I. Kuss and H. Spiesberger, Phys. Rev. **D53**, 6078 (1996).
- [19] G. Altarelli, B. Mele and F. Pitolli, Nucl. Phys. **B287**, 205 (1987).
- [20] D.J. Miller and S. Moretti, RAL-TR-1999-032 (May 1999), hep-ph/9906395; P. Lutz, talk at ECFA/DESY Linear Collider Workshop, Oxford, March 1999.